

Strongly doping dependent T_c and unconventional isotope effect of the interacting quasi-1D electron gas coupled to phonons

I. P. Bindloss

Department of Physics, University of California, Los Angeles, California 90095-1547

(Dated: February 8, 2020)

Using a multi-step renormalization group technique, the doping dependent quantum phase diagrams of the one-dimensional Hubbard-Holstein model and one-dimensional Peierls-Hubbard model are computed near half-filling, in the weak-coupling limit. In both models, the superconducting susceptibility at fixed temperature is strongly doping dependent and can exhibit a maximum, as a function of doping, at an “optimal” value of the doping. The effect of changing the ion mass on the superconducting susceptibility is found to be strongly doping dependent. The effect is largest at small dopings (near half-filling). The isotope effect on T_c in the cuprate high-temperature superconductors has a qualitatively similar doping dependence.

Recent experiments in the high-temperature superconductors suggest the presence of a strong, ubiquitous, yet unconventional electron-phonon (el-ph) interaction [1, 2]. The experiments are often analyzed in the context of the conventional theory of el-ph coupling in a Fermi liquid. However, these materials exhibit manifestly non-Fermi liquid behavior [3, 4], so the justification for this type of analysis is not clear.

The best understood non-Fermi liquid is the interacting one-dimensional electron gas (1DEG) [5]. The properties of the 1DEG coupled to phonons are dramatically different from a conventional metal coupled to phonons [6, 7, 8]. Unlike in a Fermi liquid, in 1D the el-ph interaction is strongly renormalized, and the renormalization is strongly effected by direct electron-electron (el-el) interactions. In 1D, in many cases only a small amount of retardation is necessary for a weak el-ph interaction to open a spin gap and cause a divergent superconducting susceptibility, even when the el-el repulsion is strong [8]. In contrast to BCS theory, the pairing energy and superconducting susceptibility are strongly doping dependent.

In the cuprates, both the superconducting transition temperature T_c and the isotope effect exponent $\alpha_0 = -d \ln T_c / d \ln M$, which describes changes in T_c induced by changes in the ion mass M , exhibit highly unconventional (*i.e.* non-BCS) doping dependencies. In BCS theory, T_c is only weakly dependent on the carrier concentration, and α_0 has the universal value of 1/2. In the cuprates, T_c exhibits a sharp maximum as a function of doping, and the isotope effect is not universal—it is strongly doping dependent and somewhat material dependent. α_0 is typically greater than 1 in the underdoped cuprates (indicating that, at least in this region, phonons play an important role in the superconductivity). As the doping increases, α_0 decreases, usually reaching a minimum of less than 0.1 near optimal doping [9].

The small value of α_0 at optimal doping in the cuprates likely rules out a conventional BCS-type phonon pairing mechanism. However, if the pairing mechanism is different from the BCS mechanism, it does not mean that phonons are irrelevant. In this letter we compute

α_0 for the quasi-1DEG coupled to phonons, under the assumption that charge density wave (CDW) order is dephased by spatial or dynamic fluctuations of the 1D chains [10, 11]. For many choices of the parameters, the computed α_0 has a qualitatively similar doping dependence as the α_0 measured in the cuprates: it is larger than the BCS value at small dopings, then drops below the BCS value as the doping is increased. We also show that the quasi-1DEG coupled to phonons displays a strongly doping dependent T_c that can have a sharp maximum as a function of doping. This behavior can occur despite the fact that the superconducting pairing energy, determined by the spin gap, is a monotonically decreasing function of increasing doping.

The technique we employ is the multi-step renormalization group (MSRG) method described in detail in a previous paper [8]. In this method, we start with a microscopic el-ph model and integrate out high energy degrees of freedom, via an RG transformation. This is done in multiple steps, as elaborated below. At low energies one obtains an effective field theory that is identical to that of the 1DEG (without el-ph coupling), except for renormalized values of the el-el interactions and bandwidth. MSRG treats the el-el and el-ph interactions on equal footing, takes into account retardation effects, properly treat the quantum phonon dynamics, and can be used for any band filling. The accuracy of this analytic technique in computing weak-coupling phase diagrams was demonstrated in Ref. 8 by comparison with exact numerical results. Here we shall apply it to two models of the interacting 1DEG coupled to phonons, as defined below.

The 1D Peierls-Hubbard (Pei-Hub) Hamiltonian is

$$\begin{aligned} \mathcal{H}_{\text{Pei-Hub}} = & - \sum_{i,\sigma} [t - \alpha(u_{i+1} - u_i)] (c_{i,\sigma}^\dagger c_{i+1,\sigma} + \text{H.C.}) \\ & + \sum_i \left[\frac{p_i^2}{2M} + \frac{K}{2}(u_{i+1} - u_i)^2 \right] + U \sum_i n_{i,\uparrow} n_{i,\downarrow}. \end{aligned}$$

In this model, acoustic phonons couple to electrons by modifying the bare hopping matrix element t by the el-

ph coupling strength α times the relative displacements $u_{i+1} - u_i$ of two neighboring ions [12]. The last term is the Hubbard interaction. For this model we will approximate the phonon dispersion by its value at the zone boundary of $2\sqrt{K/M} \equiv \omega_0$, since the el-ph interaction vanishes at zero momentum transfer.

The 1D Holstein-Hubbard (Hol-Hub) model is defined by the Hamiltonian

$$\mathcal{H}_{\text{Hol-Hub}} = -t \sum_{i,\sigma} (c_{i,\sigma}^\dagger c_{i+1,\sigma} + \text{H.C.}) + \sum_i \left[\frac{p_i^2}{2M} + \frac{\kappa}{2} q_i^2 \right] + g\sqrt{2M\omega_0} \sum_i q_i n_i + U \sum_i n_{i,\uparrow} n_{i,\downarrow}.$$

Here dispersionless optical phonons with coordinate q_i and frequency $\omega_0 = \sqrt{\kappa/M}$ couple to the electron density $n_i = \sum_\sigma c_{i,\sigma}^\dagger c_{i,\sigma}$ with el-ph coupling constant g [13].

It is convenient to define the dimensionless quantities

$$\lambda_{\text{Pei}} = 2N_0(\alpha \sin k_F)^2/K, \quad \lambda_{\text{Hol}} = N_0 g^2/\omega_0, \\ \bar{U} = U/(\pi v_F), \quad \delta = \ln(\mu/\omega_0)/\ln(E_F/\omega_0),$$

where $N_0 \equiv 2/(\pi v_F)$. As usual, v_F , k_F , and E_F are the Fermi velocity, momentum, and energy, respectively. (We have set \hbar and the lattice parameter equal to unity.) μ is the chemical potential measured with respect to its value at half-filling. In this letter we study the range $\omega_0 < \mu < E_F$ ($0 < \delta < 1$). The doping concentration x relative to half-filling is given by $x \approx N_0 \omega_0 (E_F/\omega_0)^\delta$. Since the MSRG method is perturbative, it is only quantitatively accurate for λ_{Pei} , λ_{Hol} , $\bar{U} \ll 1$, but is believed to be qualitatively accurate for λ_{Pei} , λ_{Hol} , $\bar{U} \sim 1$ [8].

Fig. 1 presents the phase diagrams of the above models, computed with MSRG. They are shown in the $\lambda_{\text{Hol}} - \delta$ and $\lambda_{\text{Pei}} - \delta$ planes at several fixed values of \bar{U} . The phase boundaries separate regions where various types of order have divergent susceptibilities in the low temperature limit. The susceptibility that diverges most strongly (*i.e.* dominates) is shown without parenthesis; parenthesis indicate a susceptibility that diverges less strongly. The charge sector is gapless everywhere in the phase diagrams. Above the thick solid line, the system is spin-gapped and termed a Luther-Emery liquid (LEL) [14]. Below this line, it is a gapless, quantum-critical Luttinger liquid (LL) [5]. Note that moving toward half-filling (reducing δ) increases the stability of the LEL phase relative to the LL phase in the Pei-Hub model, but has the opposite effect in the Hol-Hub model.

The thick solid line was determined by integrating out degrees of freedom between E_F and $\omega_0 < E_F$, and then requiring that the total effective backward-scattering interaction $g_1^{\text{tot}}(\omega_0) = \bar{U}/(1 + \bar{U}l_0) - \lambda_1(\omega_0)$ is zero. Here $l_0 \equiv \ln(E_F/\omega_0)$ parameterizes the amount of retardation, and $\lambda_1(\omega_0) > 0$ is the effective strength of the backward scattering (momentum transfer near $2k_F$) portion of the el-ph interaction, after integrating out states between E_F

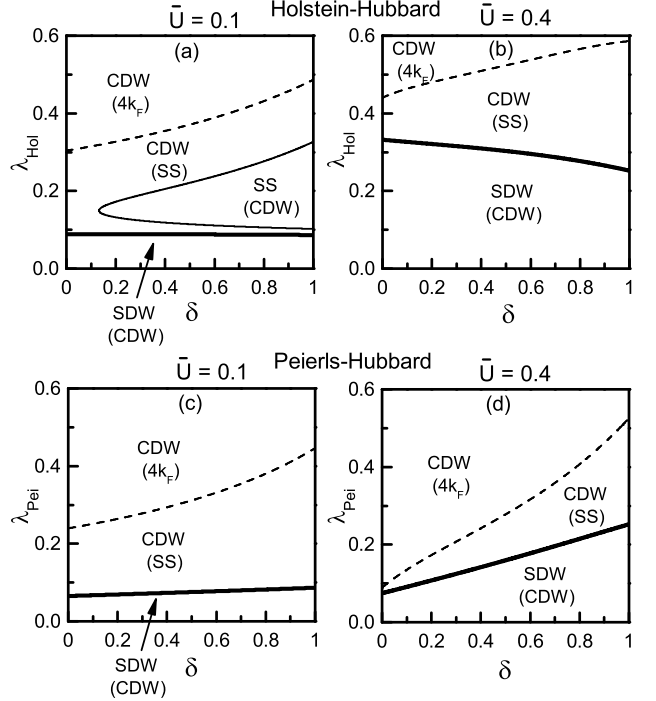


FIG. 1: Zero-temperature phase diagrams for the Hol-Hub model (panels a and b), and Pei-Hub model (panels c and d). (a) and (c) are for $\bar{U} = 0.1$; (b) and (d) are for $\bar{U} = 0.4$. For all diagrams, $E_F/\omega_0 = 5$. Parenthesis indicate a sub-dominant susceptibility. SDW stands for $2k_F$ spin density wave, CDW stands for $2k_F$ charge density wave, SS stands for singlet superconductivity, and $4k_F$ stands for $4k_F$ charge density wave. The system is spin-gapped above the thick solid line.

and ω_0 . It is determined in two steps: First, one integrates from E_F to $\mu < E_F$ using the RG flow equations that govern half-filled systems, resulting in an effective λ_1 of [8]

$$\lambda_1(\mu) = \left(\frac{\lambda_{\text{Hol}}}{1 - \lambda_{\text{Hol}} X/\bar{U}} \right) \sqrt{\frac{1 - c\bar{U}l_0}{(1 + c\bar{U}l_0)^3}} \quad (1)$$

or

$$\lambda_1(\mu) = \left(\frac{\lambda_{\text{Pei}}}{1 - \lambda_{\text{Pei}} Y/\bar{U}} \right) \sqrt{\frac{1}{[1 - (c\bar{U}l_0)^2]^3}} \quad (2)$$

for the Hol-Hub and Pei-Hub models respectively, where $X \equiv 4 \left[1 - \sqrt{(1 - c\bar{U}l_0)/(1 + c\bar{U}l_0)} \right] - 2 \arcsin(c\bar{U}l_0)$, $Y \equiv 2c\bar{U}l_0/\sqrt{1 - (c\bar{U}l_0)^2}$, and $c \equiv 1 - \delta$. Next, $\lambda_1(\mu)$ is used as the initial value to integrate from μ to $\omega_0 < \mu$, employing the RG flow equations that govern strongly incommensurate systems, resulting in [8]

$$\lambda_1(\omega_0) = \left(\frac{\lambda_1(\mu)}{1 - \lambda_1(\mu) Z/\bar{U}} \right) \sqrt{\frac{\exp(\delta\bar{U}l_0)}{(1 + \delta\bar{U}l_0)^3}} \quad (3)$$

for either model, where $Z \equiv \int_0^{\delta \bar{U} l_0} dx \sqrt{\exp(x)/(1+x)^3}$. The condition $g_1^{\text{tot}}(\omega_0) = 0$ then determines the following critical values for the microscopic el-ph couplings:

$$\lambda_{\text{Hol}}^{\text{Gap}} = \bar{U} \{ [(1 + \bar{U} l_0) S_3 + Z] / S_1 + X \}^{-1}, \quad (4)$$

$$\lambda_{\text{Pei}}^{\text{Gap}} = \bar{U} \{ [(1 + \bar{U} l_0) S_3 + Z] / S_2 + Y \}^{-1}, \quad (5)$$

where we defined $S_1 = (1 + c\bar{U} l_0)^{3/2} (1 - c\bar{U} l_0)^{-1/2}$, $S_2 = [1 - (c\bar{U} l_0)^2]^{3/2}$, and $S_3 = e^{\delta \bar{U} l_0/2} (1 + \delta \bar{U} l_0)^{-3/2}$. The system is a spin-gapped LEL for $\lambda_{\text{Hol}} > \lambda_{\text{Hol}}^{\text{Gap}}$ in the Hol-Hub model and $\lambda_{\text{Pei}} > \lambda_{\text{Pei}}^{\text{Gap}}$ in the Pei-Hub model.

In the LEL phase, the portion of the singlet superconductivity (SS) and $2k_F$ CDW susceptibility that is potentially strongly divergent as $T \rightarrow 0$ is given by $\chi_{\text{SS}} \propto \Delta_s T^{1/K_c^{\text{eff}}-2}$ and $\chi_{\text{CDW}} \propto \Delta_s T^{K_c^{\text{eff}}-2}$ respectively, where Δ_s is the spin gap, T is the temperature, and the effective charge Luttinger exponent is $K_c^{\text{eff}} = \sqrt{[2 + 2g_4^{\text{tot}} + g_c^{\text{tot}}(\omega_0)] / [2 + 2g_4^{\text{tot}} - g_c^{\text{tot}}(\omega_0)]}$. Here $g_c^{\text{tot}}(\omega_0) = -\bar{U}/(1 - c\bar{U} l_0) - \lambda_1(\omega_0) + 2\lambda_2$ and $g_4^{\text{tot}} = \bar{U}/2 - \lambda_2$, where the forward scattering el-ph interaction λ_2 is given by $\lambda_2 = \lambda_{\text{Hol}}$ for the Hol-Hub model and $\lambda_2 = 0$ for the Pei-Hub model. For the case $-1 < g_1^{\text{tot}}(\omega_0) < 0$, $\Delta_s = \omega_0 e \exp[-1/|g_1^{\text{tot}}(\omega_0)|]$ [8]. For $g_1^{\text{tot}}(\omega_0) > 0$, $\Delta_s = 0$.

The thin solid line in Fig. 1a is determined by $K_c^{\text{eff}} = 1$, which leads to the following critical values for λ_{Hol} :

$$\lambda_{\text{Hol}}^{\text{SS},\pm} = \bar{U} \left[B \pm \sqrt{B^2 - S_1 A C / 2} \right], \quad (6)$$

where $A = (S_1 X + Z)^{-1}$, $B = [(2S_1 - S_3)A + C]/4$, and $C = (1 - c\bar{U} l_0)^{-1}$. The SS susceptibility is the dominant one if $K_c^{\text{eff}} > 1$, which occurs if the two conditions $S_1 A C < 2B^2$ and $\lambda_{\text{Hol}}^{\text{SS},-} < \lambda_{\text{Hol}} < \lambda_{\text{Hol}}^{\text{SS},+}$ are met. The thin solid line is absent in Fig. 1b because $S_1 A C > 2B^2$ everywhere. This line is always absent in the Pei-Hub model with $\bar{U} > 0$, because then $K_c^{\text{eff}} < 1$ always.

The dashed lines in Fig. 1 are determined by the critical el-ph coupling strengths

$$\lambda_{\text{Hol}}^{\text{CDW}} = \bar{U} \left[D + \sqrt{D^2 + 5S_1 A E / 4} \right], \quad (7)$$

$$\lambda_{\text{Pei}}^{\text{CDW}} = \bar{U} \{ (S_3/E + Z) / S_2 + Y \}^{-1}, \quad (8)$$

where $D = A[S_1(4 - 5EX) - 5(EZ + S_3)]/8$ and $E = (6/\bar{U} + 3)/5 - C$. If $\lambda_{\text{Hol}} > \lambda_{\text{Hol}}^{\text{CDW}}$ for the Hol-Hub model, or if $\lambda_{\text{Pei}} > \lambda_{\text{Pei}}^{\text{CDW}}$ for the Pei-Hub model, then $K_c^{\text{eff}} < 1/2$, which means that SS is not divergent.

Examining Fig. 1d, we see that for moderate values of λ_{Pei} , for example near $\lambda_{\text{Pei}} \approx 0.2$, χ_{SS} is not divergent near $\delta = 0$, where $K_c^{\text{eff}} < 1/2$, nor is it divergent near $\delta = 1$, where $\Delta_s = 0$. However, χ_{SS} is divergent for a certain range of moderate δ . Therefore, in these cases, at fixed $T \ll \Delta_s$, χ_{SS} exhibits a peak as a function of δ at an intermediate value of δ . This peak is shown explicitly in Figs. 2 and 3, where we

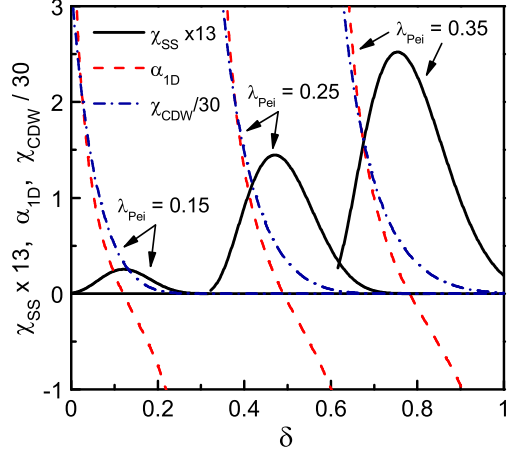


FIG. 2: Doping dependence of the singlet superconducting susceptibility χ_{SS} (solid lines), 1D isotope effect exponent α_{1D} (dashed lines), and $2k_F$ CDW susceptibility χ_{CDW} (dash-dotted lines), for the Pei-Hub model with $\bar{U} = 0.4$, $E_F/\omega_0 = 5$, and $T/\omega_0 = 0.1$. The curves are shown for $\lambda_{\text{Pei}} = 0.15, 0.25$, and 0.35 .

plot $\chi_{\text{SS}} \equiv (\Delta_s/E_F)(T/E_F)^{1/K_c^{\text{eff}}-2}$ (thick solid line) versus δ at $T/\omega_0 = 0.1$, for representative parameters. The CDW susceptibility $\chi_{\text{CDW}} \equiv (\Delta_s/E_F)(T/E_F)^{K_c^{\text{eff}}-2}$ (dash-dotted lines) does not exhibit such a peak.

In Fig. 3 we plot Δ_s/ω_0 (thin solid lines), which shows that at low dopings, χ_{SS} increases with increasing doping, despite that the superconducting pairing strength Δ_s decreases! In the cuprates, the superconducting gap also decreases with increasing doping, which in the underdoped region occurs at the same time that T_c increases! Note that for an array of weakly coupled quasi-1D chains, assuming CDW order is dephased, a peak in χ_{SS} as a function of δ , at fixed temperature, implies that T_c exhibits a peak at that same δ (assuming the interchain coupling is doping independent).

Before investigating α_{1D} for a quasi-1D array of chains, we compute the purely 1D isotope effect exponent $\alpha_{\text{1D}} \equiv -d \ln \chi_{\text{SS}} / d \ln M$ [15]. The analogous quantity in BCS theory is $\alpha_{\text{BCS}} \equiv -d \ln \chi_{\text{BCS}} / d \ln M = [2 \ln(\gamma \omega_0 / T)]^{-1}$. Here the BCS superconducting susceptibility is $\chi_{\text{BCS}} = N_0 \ln(\gamma \omega_0 / T)$, where N_0 is the density of states at the Fermi energy, $\gamma = 1.13$, and $\omega_0 \propto M^{-1/2}$ is the Debye frequency. (T_c is determined by $V \chi_{\text{BCS}} = 1$ where V is the phonon induced attraction between electrons.)

The exponent α_{1D} is shown versus δ in Figs. 2 and 3 (dashed lines) at fixed T . Clearly α_{1D} depends strongly on both the doping level and interaction strengths. In contrast, α_{BCS} is independent of the carrier concentration and el-ph interaction strength; for the temperature used in the figures, $\alpha_{\text{BCS}} \approx 0.2$. At low dopings, α_{1D} is larger than α_{BCS} , then decreases rapidly with increasing δ , eventually dropping below α_{BCS} .

For an array of weakly coupled quasi-1D chains with

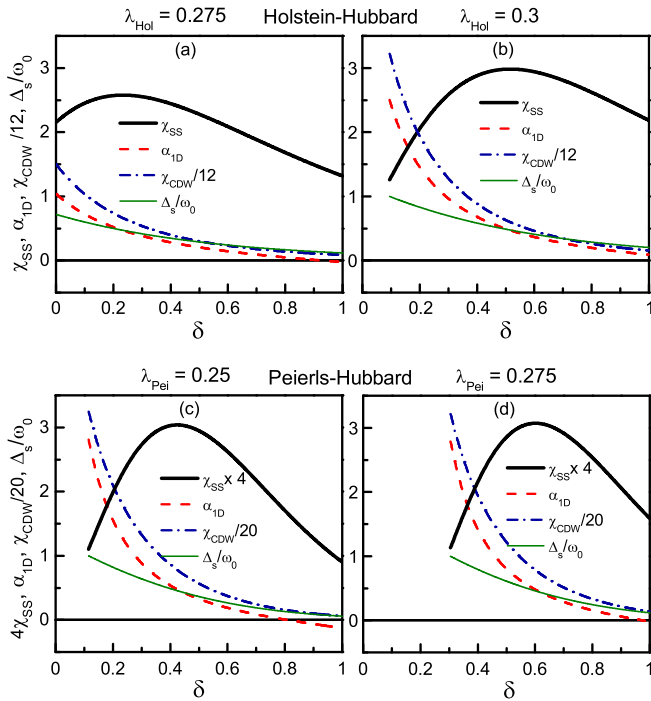


FIG. 3: Doping dependence of χ_{ss} (thick solid lines), α_{1D} (dashed lines), χ_{CDW} (dash-dotted lines), and Δ_s/ω_0 (thin solid lines), for the Hol-Hub model (panels a and b), and the Pei-Hub model (panels c and d). All curves were computed for $\bar{U} = 0.1$, $E_F/\omega_0 = 5$, and $T/\omega_0 = 0.1$. The values of λ_{Hol} and λ_{Pei} are labeled above each plot.

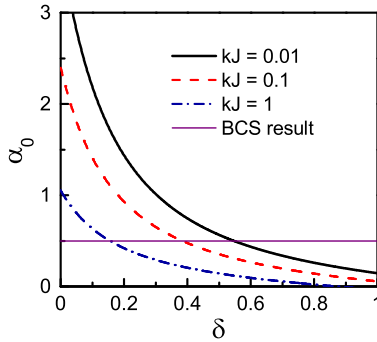


FIG. 4: Doping dependence of the isotope effect exponent α_0 for a quasi-1DEG with $E_F/\omega_0 = 5$, $\bar{U} = 0.1$, $\lambda_{Hol} = 0.275$, and various values of the interchain coupling kJ . The BCS result $\alpha_0 = 1/2$ is also shown.

dephased CDW, the isotope effect exponent α_0 has a qualitatively similar doping dependence as α_{1D} . We demonstrate this by treating the interchain coupling on a mean-field level [16, 17], which means that T_c is determined by the temperature at which $kJ\chi_{ss} = 1$, where k is a constant and J is the interchain coupling. In Fig. 4, we show α_0 versus δ for various fixed values of kJ , for the same interaction strengths as Fig. 3a. At low dopings, α_0 is larger than the BCS value, then drops below 1/2 as

δ is increased.

In some models [16] of high-temperature superconductivity based on stripes [18], the concentration of holes on a stripe remains fixed when the doping of the material changes, but the spacing between the stripes changes. In that case, as the doping increases, the parameter δ remains fixed but J increases due to the decreased spacing between stripes. Then Fig. 4 predicts that α_0 again decreases with increasing doping. In such a model, in the underdoped region, where the stripes are far apart and represent well defined quasi-1D electron gases, increasing the doping increases T_c due to the increase in J . But in the overdoped region, the stripes begin to lose their 1D character. This necessarily drives T_c down since their quasi-1D character was the reason for the high pairing scale in the first place.

To conclude, in at least one non-Fermi liquid, the interacting 1DEG, the attractive interaction mediated by phonons can cause a strongly divergent superconducting susceptibility with properties that are dramatically different from a Fermi liquid superconductor. Therefore, if a superconductor displays properties that are different from BCS theory, one should never use this, in and of itself, to argue that the pairing mechanism is non-phonon.

It is a pleasure to acknowledge useful discussions with S. Kivelson. This work was supported by the Department of Energy contract No. DE-FG03-00ER45798.

- [1] A. Lanzara *et al.*, Nature (London) **412**, 510 (2001); X. J. Zhou *et al.*, Nature (London) **423**, 398 (2003).
- [2] J.-H. Chung *et al.*, Phys. Rev. B **67**, 014517 (2003).
- [3] T. Valla *et al.*, Science **285**, 2110 (1999).
- [4] I. P. Bindloss and S. A. Kivelson, cond-mat/0402457.
- [5] For reviews see V. J. Emery, in *Highly Conducting One-Dimensional Solids*, edited by J. T. Devreese, R. P. Evrard, and V. E. van Doren (Plenum, New York, 1979); J. Voit, Rep. Prog. Phys. **58**, 977 (1995).
- [6] G. T. Zimanyi *et al.*, Phys. Rev. Lett. **60**, 2089 (1988).
- [7] J. Voit, Phys. Rev. Lett. **64**, 323 (1990).
- [8] I. P. Bindloss, cond-mat/0404154.
- [9] Isotope effects in the cuprates are reviewed in Guo-meng Zhao *et al.*, J. Phys.: Condens. Matter **13**, R569 (2001).
- [10] V. J. Emery *et al.*, Phys. Rev. B **56**, 6120 (1997).
- [11] S. A. Kivelson *et al.*, Nature (London) **393**, 550 (1998).
- [12] W. P. Su *et al.*, Phys. Rev. Lett. **42**, 1698 (1979).
- [13] T. Holstein, Ann. Phys. (NY) **8**, 343 (1959).
- [14] A. Luther and V. J. Emery, Phys. Rev. Lett. **33**, 589 (1974).
- [15] To compute this quantity, one can use $\alpha_{1D} = -\frac{1}{2} \frac{\Delta\chi_{ss}/\chi_{ss}}{\Delta\xi/\xi}$, where $\xi \equiv E_F/\omega_0 = e^{l_0}$ and $\Delta\chi_{ss} = \chi'_{ss} - \chi_{ss}$. Here χ'_{ss} is the result for the SS susceptibility after changing $l_0 \rightarrow l'_0 = \ln(\xi + \Delta\xi)$, $c \rightarrow c' = c l_0/l'_0$, and $\delta \rightarrow 1 - c'$, where $\Delta\xi$ is infinitesimal.
- [16] E. W. Carlson *et al.*, Phys. Rev. B **62** 3422 (2000).
- [17] E. Arrigoni *et al.*, cond-mat/0309572.
- [18] S. A. Kivelson *et al.*, Rev. Mod. Phys. **75**, 1201 (2003).